PHYSICAL REVIEW B **80**, 081303(R) (2009)

Exciton localization and migration in individual CdSe quantum wires at low temperatures

J. J. Glennon, R. Tang, W. E. Buhro, and R. A. Loomis*
Department of Chemistry and Center for Materials Innovation, Washington University in St. Louis, One Brookings Drive, CB 1134, St. Louis, Missouri 63130, USA

D. A. Bussian, H. Htoon, and V. I. Klimov†
Chemistry Division and Center for Integrated Nanotechnologies, Los Alamos National Laboratory, Los Alamos, New Mexico 87545, USA

(Received 13 June 2009; published 11 August 2009)

Low-temperature (<40 K) photoluminescence (PL) spectra of individual CdSe nanocrystal quantum wires exhibit narrow (<5 meV) isolated peaks spanning a range ≤50 meV. We attribute these features to emission of excitons localized in shallow (a few meV deep) tight potential minima superimposed on longer-scale and larger-amplitude variations of the potential energy. Spectrally resolved PL dynamics reveal decreasing exciton-decay rates with decreasing emission energy. These observations are consistent with exciton relaxation within a manifold of localization sites characterized by an exponential density of states.

DOI: 10.1103/PhysRevB.80.081303 PACS number(s): 78.67.Lt, 78.55.Qr, 78.67.Hc

The ability to manipulate energy flows in nanoscale materials is an important goal of current research across a range of disciplines from physics to biology. In nature, rapid funneling of electronic excitations to a reaction center enabled by dipole-dipole interactions is a critical component of photosynthesis.[1] Further, efficient energy transfer (ET) mediated by electrostatic interactions has been observed in a variety of organic materials including porphyrins,[2] conjugated polymers,[3] and biomolecules.[4] A recent approach to controlling energy flow over nanoscale lengths involves the use of assemblies of semiconductor nanocrystal quantum dots (NQDs).[5,6] Here, the advantages are well-defined and tunable energy structures of NQDs that allow for precise engineering of spectral overlap in donor-acceptor pairs.

Nanocrystal quantum wires (NQWs) are a unique class of one-dimensional (1D) nanomaterials synthesized using colloidal techniques[7–9] that can also allow for facile manipulation of energy flow on the nanoscale. These NQWs can be synthesized with sufficiently small diameters to give rise to quantum confinement in the radial dimension, and, as in NQDs, the electronic spectra of NQWs can be tuned by varying the wire diameter. The large lengths attainable in NQWs, >10 μm, can allow for low-loss transport of charges or excitons across large distances. Potentially, this could yield significant increases in the efficiency of electronic and optoelectronic devices including solar cells. The ability to control charge or exciton flows, perhaps by varying the diameter or chemical composition of the NQW, would further enhance the utility of these materials.

In this Rapid Communication, we report photoluminescence (PL) studies on individual CdSe NQWs that demonstrate distinct signatures of intrawire exciton transfer within a manifold of shallow localized states. Specifically, we present spectrally and temporally resolved PL results obtained at room and low, 4–40 K, temperatures (abbreviated as RT and LT, respectively). We observe narrow lines in LT PL at low-pump intensity. However, these features wash out with increasing temperature or excitation power density. Spatially resolved PL spectra indicate that these narrow lines arise from localized spatial regions along the NQW. Time- and wavelength-resolved LT PL data show spectrally heterogeneous dynamics characterized by decay rates that decrease with decreasing emission energy. These observations are consistent with exciton migration via ET from higher- to lower-energy localized states.

CdSe NQWs with a mean diameter of 9.2 ± 1.1 nm (determined via transmission electron microscopy; Ref. 16) were prepared by the solution-liquid-solid method.[7–9] Dilute solutions of NQWs in toluene were drop cast onto a crystalline quartz substrate. For wide-field imaging and steady-state PL spectroscopy, the NQWs were excited using 2.33 eV photons from a continuous-wave (cw) diode laser with a power density of ~0.2 W cm^{-2}. Time-resolved PL studies were conducted using the 2.33 eV output from a pulse-picked intracavity doubled parametric oscillator (150 fs pulse duration) pumped by a mode-locked Ti:sapphire laser. The pump fluence was approximately 5 μJ cm^{-2}, which corresponded to the generation of <20 excitons within the ~2 μm diameter excitation spot. The role of multiparticle effects (e.g., Auger recombination) should be insignificant for this excitation density as the average separation between excitons is much greater than the Bohr exciton radius. PL from single NQWs was collected using a 40X microscope objective and imaged onto the entrance slit of a 0.5 m spectrometer. Time-resolved PL with 400 ps temporal resolution was acquired via time-correlated single-photon counting (TCSPC).

The peak in the RT PL spectrum of an ensemble NQW sample is ~1.75 eV. This PL peak is slightly below the lowest-energy absorption feature, 1.79 eV, indicating that it is due to intrinsic band-edge emission typically associated with recombination of electron-hole pairs bound into 1D excitons.[10] The available literature data suggest that the exciton binding energy in 1D CdSe nanostructures is at least 30 meV,[11] and hence, excitons are stable (i.e., do not dissociate) up to RT. The maxima in the RT PL spectra of single CdSe NQWs [Fig. 1(a); top spectrum] are nearly the same as those in ensemble spectra and fall between 1.75–1.77 eV. Furthermore, the PL spectra recorded at different positions along a 4.0-μm-long NQW with ~1 μm resolution are spatially uniform and do not vary with time.

The PL spectra of single CdSe NQWs recorded at LT (4 K) using low-power cw excitation are distinctly different

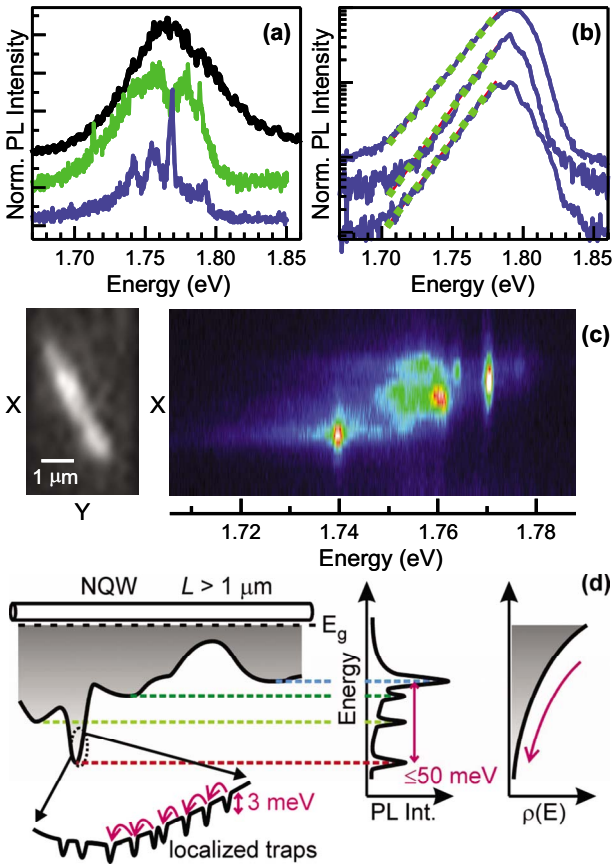

FIG. 1. (Color online) (a) PL spectra of individual CdSe NQWs recorded at temperatures of 4 K (blue; bottom trace), 40 (green; middle trace), and 300 K (black; top trace) using cw excitation with a power density of ~0.2 W cm^{-2}. (b) PL spectra of three different NQWs at 4 K excited with 150 fs pulses at 532 nm and per-pulse fluences of ~5 $\mu J\ cm^{-2}$. The green dotted lines are single-exponential fits of the low-energy tail. (c) PL spectra recorded as a function of position along the NQW shown on the left; cw excitation was used, and the temperature was 4 K. (d) Left: schematic of the potential-energy landscape in a CdSe NQW: shallow traps are superimposed on top of larger-amplitude variations of potential energy. Middle: at LT and low excitation power levels, emission from excitons localized in shallow traps gives rise to sharp energetically distinct peaks. Right: the low-energy tail of the high-pump-intensity PL spectrum reflects an energetic distribution of trap sites in these NQWs that decays exponentially with decreasing energy.

from those at RT and contain narrow discrete features [Fig. 1(a); bottom spectrum] that develop likely as a result of exciton localization in potential minima (exciton trap sites). Signatures of spatial localization are also evident in spectrally resolved images of NQWs [Fig. 1(c)], which indicate that the PL intensity concentrates in bright spots producing distinctly different emission spectra. As the temperature is raised above 30–40 K, discrete spectral features widen and merge together [Fig. 1(a); middle spectrum], eventually forming a broad band that is similar to that observed at RT [Fig. 1(a); top spectrum]. The increase in temperature is also accompanied by smearing out spatial nonuniformity in PL intensity.

The above temperature-dependent trends are consistent with thermal depopulation of exciton traps and further suggest that these traps are relatively shallow and characterized by a depth of only 2–3 meV. When high-excitation energy densities are implemented using pulsed-laser excitation, the sharp PL features in the LT spectra are again observed to merge into a single broad band [Fig. 1(b)]. In this case, the broadening is attributed to progressive filling of available trap sites.

The LT PL spectra also provide signatures of larger-amplitude (<50 meV) variations in the potential-energy landscape along the wire. Most of the single-NQW spectra contain not just one but several sharp PL peaks distributed in energy up to 50 meV [Fig. 1(a); bottom spectrum]. The coexistence of energetically distinct PL features in single-NQW spectra suggests that the deep potential minima are sufficiently separated in space so that exciton relaxation cannot occur between them at LT. The existence of long-scale variations in potential energy is evident from spectrally resolved NQW images [see, e.g., Fig. 1(c)], which indicate that the spatial regions producing distinct discrete PL lines can be separated by more than 1 μm.

Based on the above findings, we propose the following model for describing the potential-energy landscape in NQWs [Fig. 1(d)]. The NQW potential is comprised of closely spaced shallow (<3 meV) minima (exciton traps) riding on top of larger-amplitude (~50 meV) variations in potential energy. Shortly after excitation, a photogenerated exciton relaxes into the nearest shallow potential minimum. At LT (<40 K), exciton transport is not efficient as it typically relies on short-range tunneling.[12] In this case, the exciton can only sample a few localization sites in its immediate vicinity (within the tunneling distance) before it recombines. As a result, the low-pump-intensity LT PL spectra develop a series of sharp peaks whose energies are close to those of initially populated traps.

As the temperature increases, excitons become more mobile due to the increased efficiency of processes such as thermally activated hopping[13] and coherent transport via higher-energy delocalized states. As a result, excitons can sample both localized and delocalized states across a wider range of energies than at LT, which leads to the smearing out of discrete "localization" features in PL. Similarly, the LT PL spectra broaden and become structureless with increasing pump levels as shallow traps are filled and the probability of finding excitons in higher-energy delocalized states increases.

Within the above model, the low-energy tail of the PL spectrum measured at high intensity reflects the distribution of localized states. Interestingly, the shape of this tail is similar for different nanowires, as shown in Fig. 1(b), suggesting that the energy distribution of exciton traps does not significantly vary across the NQW ensemble. Further, we observe that the low-energy PL tail can be accurately described by an exponential dependence, $\exp(-E/E_0)$, where E is the emission energy and E_0 is the characteristic energy equal to 18 ± 3 meV [green dotted lines in Fig. 1(b)]. This type of exponential density of states, referred to as an Urbach tail, has been observed previously in both bulk and low-dimensional semiconductors.[14]

To detect signatures of exciton transport within a NQW, we conduct spectrally and temporally resolved PL studies on

individual nanowires. Exciton migration from higher- to lower-energy states is expected to lead to spectrally nonuniform PL dynamics.[5,6] At RT, PL transients have rise times limited by the instrument response and show decay, which is nearly single exponential with a time constant of ~450 ps (determined taking into account the instrument response function), independent of emission energy. Since these NQWs have very low PL quantum yields, the measured recombination rate is dominated by nonradiative processes, which likely involve surface defects. As in the case of CdSe NQDs, such defects are probably associated with unpassivated Cd and Se dangling bonds.[15] The lack of discernable spectral dependence on either PL buildup or decay is likely at RT because exciton relaxation within available states (exciton thermalization) is faster than the resolution of our measurements.

The PL transients recorded at LT indicate exciton dynamics that are considerably different from those at RT. Once the temperature is reduced below ~40 K, the transient data indicate the presence of several preferred emission energies or PL peaks, consistent with the LT PL spectra acquired with cw excitation [Fig. 1(a)]. Typical data for a single CdSe NQW held at 4 K are shown in Fig. 2(a); the plot comprises 39 decay curves recorded at different energies spanning the entire emission spectrum. The time-dependent PL spectra acquired at these lower temperatures [Fig. 2(b)] show a distinct ~13 meV shift of the emission maximum to lower energy after a delay of 9 ns from excitation. This dynamic PL shift is consistent with ET due to exciton migration from higher- to lower-energy states. While not resolvable at high temperature, ET is clearly seen at LT due to the reduced efficiency of exciton transport via mechanisms involving thermal activation. This slows down exciton migration and makes it "traceable" with sub-ns resolution of our measurements.

The PL transients recorded at the five different emission energies indicated by the arrows (labeled 1–5) in Fig. 2(a) are plotted in Fig. 2(c). The rise and decay times of the PL intensity at higher energies are shorter than those at lower energies. To quantify ET rates and derive the spectral dependence of states involved in the ET process, we analyze spectrally resolved PL transients in terms of $1/e$ relaxation times.[16] Typical $1/e$ lifetimes obtained on single NQWs increase from ~700 ps to >3 ns with decreasing emission energy. In the analysis of the ET process, it is convenient to separate the contribution due to exciton population decay from that due to exciton transfer (population spectral redistribution). The population decay can be extracted from the measured data by spectrally integrating the PL intensity measured for different delay times after excitation. By further normalizing the temporally resolved TCSPC data acquired at each emission energy by the population dynamics derived above, the dynamics due only to spectral migration of excitons can be extracted.[6,17]

This normalization yields profiles that represent the *relative* exciton populations at the different energies as a function of time [Fig. 2(d)]. At higher emission energies, 1.818 eV (purple curve; labeled as 5), the relative number of excitons quickly grows in and decays slowly after 0.4 ns. The relative number of excitons at energies near the PL peak, 1.780 eV (green curve; 3), remains fairly constant for more than 9 ns.

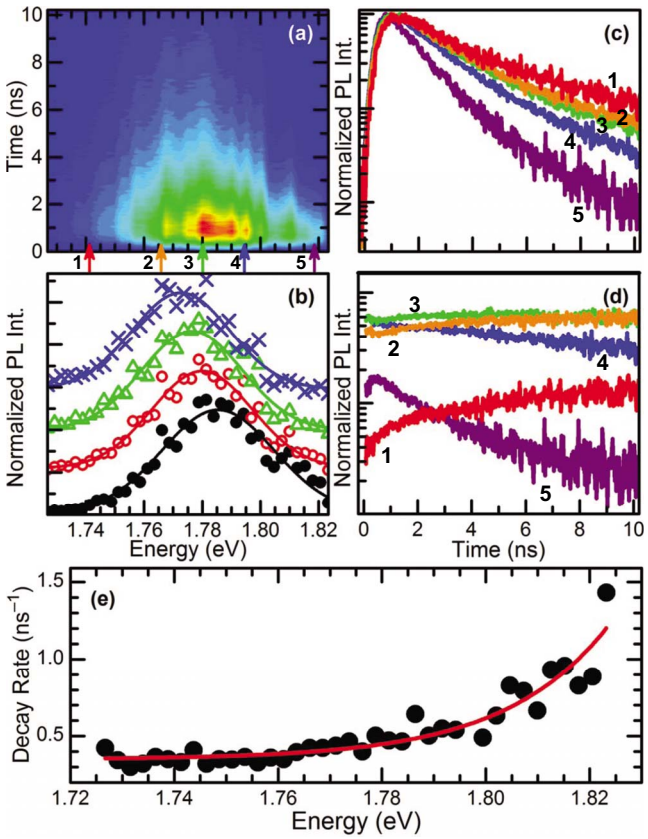

FIG. 2. (Color online) (a) A false-color plot of time- and spectrally resolved LT PL intensity from a single CdSe NQW; the PL intensity increases from blue to red. (b) Normalized PL spectra measured at different times after excitation; and 0 (black circles), 2 (red open circles), 5 (green triangles), and 9 ns (blue ×'s). The solid lines are Gaussian fits. These spectra indicate a dynamic shift of the PL to lower energy with time. (c) PL-decay curves recorded at different emission energies: 1.818 (purple; 5), 1.794 (blue; 4), 1.780 (green; 3), 1.766 (orange; 2), and 1.741 eV (red; 1). The curves are normalized to the peak intensity. (d) The same PL-decay curves as those plotted in (b) but corrected for recombination losses to reveal the ET dynamics (see text for details). (e) The $1/e$ PL-decay rates plotted as a function of detection energy (symbols) derived from the TCSPC data. The solid line is a fit using the Urbach-tail model discussed in the text with $\Gamma_p = 0.35$ ns^{-1}, $E_m = 1.805$ eV, and $E_0 = 20$ meV.

In contrast, the relative number of excitons continues to grow in at lower energies, 1.741 eV (red curve; 1), throughout the whole observation period. These temporal profiles verify that excitons undergo ET from higher-energy to lower-energy states on time scales out to at least 9 ns. The observation that the signatures of ET and the sharp "localization" features in the PL spectra both disappear at temperatures above 30–40 K indicates that exciton migration occurs within the manifold of shallow trap sites. The mechanism for exciton transport at $T < 40$ K likely involves elastic or inelastic (phonon-assisted) tunneling as observed in previous LT studies of exciton dynamics in disordered structures.[18]

We propose a simple model that incorporates an Urbach-tail distribution of localized states shown in Fig. 1(d) to model the ET data. At LT, the excitons that are trapped in

higher-energy shallow potential minima can undergo ET to a lower-energy adjacent trap within the same large-scale potential minima [indicated by the arrows in Fig. 1(d)]. For localized excitons at energy E, the ET rate (Γ_{ET}) is proportional to the number of states having energy $E' < E$, which can be calculated from $\int_0^E \rho(E')dE' = \exp[(E-E_g)/E_0]$, where E_g is the band-gap energy and E_0 defines the decay constant of the single-exponential Urbach tail [Fig. 1(d)].[19] By introducing an energy E_m where the rate of exciton population decay (Γ_p) is equal to Γ_{ET}, we obtain $\Gamma_{ET}(E)=\Gamma_p \cdot \exp[(E-E_m)/E_0]$. This then yields the following expression for the total exciton-decay rate at a given energy E: $\Gamma(E)=\Gamma_{ET}(E)+\Gamma_p=\Gamma_p \cdot (1+\exp[(E-E_m)/E_0])$. This expression has been used previously to describe ET in semiconductor quantum wells.[19–21]

The $1/e$-decay rates extracted from the TCSPC PL data in Fig. 2(a) fit very well to the model, as shown in Fig. 2(e). The best fit of the rates yields $\Gamma_p = 0.35 \pm 0.02$ ns^{-1}, $E_m = 1.805 \pm 0.003$ eV, and $E_0 = 20 \pm 3$ meV. The value of E_0 derived from PL dynamics is remarkably similar to that determined by fitting the slope of the low-energy tail in the PL spectra in Fig. 1(b) (18 meV). This agreement supports the conclusion that the observed dynamics are due to exciton migration within the manifold of shallow traps sites that are characterized by the Urbach-tail-like density of states.

To summarize, sharp features in the PL spectra and energy-dependent exciton-decay rates within single NQWs at temperatures below 30–40 K indicate that excitons become localized in shallow (2–3 meV deep) closely separated traps and subsequently can undergo ET between these potential minima. The shallow traps are superimposed on larger length scale, higher-amplitude ($\leq$50 meV) potential undulations, which lead to the development of multiple sharp PL peaks (separated by up to tens of meV) in single-wire PL spectra. The potential variations along the wire can be produced by a number of mechanisms. One possibility is associated with fluctuations of the wire diameter; the formation of localized minima attributed to fluctuations in the thickness of two-dimensional semiconductor quantum well has been extensively studied.[22] Variations in the crystal structure along the NQWs,[10,23] inhomogeneities in surface coverage by ligand molecules, nonuniform electrostatic environments, and interactions with the substrate may also contribute to the potential fluctuations.

This work was supported by the David and Lucile Packard Foundation, the National Science Foundation (Grant No. CHE-0518427), the Center for Materials Innovation at Washington University, and the Chemical Sciences, Biosciences, and Geosciences Division of the Office of Basic Energy Sciences, Office of Science, U.S. Department of Energy (DOE). Single-NQW measurements were conducted at the Center for Integrated Nanotechnologies (CINT) operated jointly for DOE by Los Alamos and Sandia National Laboratories as part of the CINT user program.

*loomis@wustl.edu

†klimov@lanl.gov

[1] D. Gust, T. A. Moore, and A. L. Moore, Acc. Chem. Res. **34**, 40 (2001).

[2] G. Kodis *et al.*, J. Phys. Chem. A **106**, 2036 (2002).

[3] D. Beljonne *et al.*, Proc. Natl. Acad. Sci. U.S.A. **99**, 10982 (2002).

[4] L. Stryer, Annu. Rev. Biochem. **47**, 819 (1978).

[5] S. A. Crooker, J. A. Hollingsworth, S. Tretiak, and V. I. Klimov, Phys. Rev. Lett. **89**, 186802 (2002).

[6] M. Achermann *et al.*, J. Phys. Chem. B **107**, 13782 (2003).

[7] H. Yu *et al.*, J. Am. Chem. Soc. **125**, 16168 (2003).

[8] H. Yu *et al.*, Nature Mater. **2**, 517 (2003).

[9] F. Wang *et al.*, Inorg. Chem. **45**, 7511 (2006).

[10] V. V. Protasenko, K. L. Hull, and M. Kuno, Adv. Mater. **17**, 2942 (2005).

[11] A. Shabaev and Al. L. Efros, Nano Lett. **4**, 1821 (2004); N. Le Thomas, E. Herz, O. Schops, and U. Woggon, Phys. Rev. Lett. **94**, 016803 (2005).

[12] T. Takagahara, Phys. Rev. B **31**, 6552 (1985).

[13] D. Monroe, Phys. Rev. Lett. **54**, 146 (1985).

[14] F. Urbach, Phys. Rev. **92**, 1324 (1953).

[15] V. I. Klimov, D. W. McBranch, C. A. Leatherdale, and M. G. Bawendi, Phys. Rev. B **60**, 13740 (1999).

[16] See EPAPS Document No. E-PRBMDO-80-R25928 for the determination of a mean diameter of the NQWs and the analysis of PL dynamics in terms of a double-exponential decay. For more information on EPAPS, see http://www.aip.org/pubservs/epaps.html

[17] This procedure assumes that the donor and the acceptor states emit at distinctly different spectral energies, and the rate for nonradiative exciton recombination is not dependent on energy.

[18] E. Cohen and M. D. Sturge, Phys. Rev. B **25**, 3828 (1982).

[19] M. Oueslati, C. Benoitala Guillaume, and M. Zouaghi, Phys. Rev. B **37**, 3037 (1988).

[20] C. Gourdon and P. Lavallard, Phys. Status Solidi B **153**, 641 (1989).

[21] C. Gourdon and P. Lavallard, J. Cryst. Growth **101**, 767 (1990).

[22] D. Gammon, E. S. Snow, B. V. Shanabrook, D. S. Katzer, and D. Park, Phys. Rev. Lett. **76**, 3005 (1996).

[23] J. J. Glennon *et al.*, Nano Lett. **7**, 3290 (2007).